Int J Clin Exp Med 2018;11(8):8018-8024
www.ijcem.com /ISSN:1940-5901/IJCEM0068862

Original Article

Differentiating hepatic metastases of gastroenteropancreatic neuroendocrine cancer and adenocarcinoma using enhanced CT

Yong Cui[1], Xiao-Ting Li[1], Jie Li[2], Zhong-Wu Li[3], Yan-Jie Shi[1], Hui-Ci Zhu[1], Ying-Shi Sun[1]

Departments of [1]Radiology, [2]Gastrointestinal Oncology, [3]Pathology, Key Laboratory of Carcinogenesis and Translational Research (Ministry of Education), Peking University Cancer Hospital & Institute, Beijing, China

Received November 9, 2017; Accepted April 18, 2018; Epub August 15, 2018; Published August 30, 2018

Abstract: Recent studies have demonstrated that dynamic enhanced CT has potential for distinguishing gastroenteropancreatic neuroendocrine cancer (GEP-NEC) from gastroenteropancreatic adenocarcinoma (GEP-ADC). However, little is known about the performance of CT in differentiating hepatic metastases of those tumors. We therefore aimed to assess the capability of contrast-enhanced CT to differentiate between GEP-NEC and GEP-ADC hepatic metastases. CT images of 33 cases of GEP-NEC hepatic metastases and 33 cases of GEP-ADC hepatic metastases were retrospectively reviewed. Qualitative analysis included tumor distribution, the presence or absence of tumor-feeding arteries and intratumoral neovascularity, and dynamic enhancement patterns. Quantitative analysis included tumor size, tumor number, measurement of CT attenuation of tumors and adjacent liver parenchyma, and calculation of the enhancement ratio of the lesion versus the surrounding liver in the hepatic arterial phase (T-L/A) and portal venous phase. There was a significantly higher prevalence of tumor feeding arteries (72.7% vs. 36.4%, p=0.003) and intratumoral neovascularity (57.6% vs. 12.1%, p<0.001) and less plateau enhancement (42.4% vs. 84.8%, p=0.002) in GEP-NEC hepatic metastases than GEP-ADC hepatic metastases. The mean T-L/A in GEP-NEC hepatic metastases was significantly higher compared to GEP-ADC hepatic metastases (0.90±0.24 vs. 0.72±0.19, p=0.001). Regression analysis identified the presence of intratumoral neovascularity as the only independent predictor of GEP-NEC hepatic metastases on CT (odds ratio=7.097; 95% CI=1.852-27.196; p=0.004). Together, these results suggest that contrast-enhanced CT may have clinical application in the differential diagnosis of hepatic metastases from GEP-NEC or GEP-ADC.

Keywords: Gastroenteropancreas neuroendocrine tumor, adenocarcinomas, tomography, X-Ray computed, differential diagnosis

Introduction

Neuroendocrine cancers (NECs) are the second most prevalent cancer of the gastroenteropancreatic (GEP) tract, and incidence has been increasing in recent years [1, 2]. The World Health Organization defines NEC as a neuroendocrine tumor that contains cells with greater than a 20% Ki-67 labeling index. Most GEP-NECs are diagnosed in the advanced stage and involve metastases to the liver [3, 4]. Notably, the presence of hepatic metastases is one of the most powerful predictors of poor prognosis in GEP-NEC [5, 6].

Hepatic metastases are also prevalent in other cancers of the GEP, including GEP adenocarcinoma (ADCs). Understanding the pathological differences in GEP-NECs and GEP-ADCs has important treatment implications, as NECs and ADCs are treated with different systemic chemotherapy regimens. First-line systemic chemotherapy with cisplatin and etoposide is recommended for most patients with GEP-NEC and metastases [7]. However, this regimen is not appropriate for GEP-ADCs. Therefore, understanding the differential pathology of GEP-NEC and GEP-ADC at diagnosis and treatment initiation is essential for clinical decision making.

Computed tomography (CT) is used to assess the primary tumor and the extent of distant spread to facilitate decisions regarding the opti-

Table 1. Case material

	NEC hepatic metastases (n=33)	ADC hepatic metastases (n=33)
Age (Mean ± SD)	61.39±9.22	61.94±8.50
Sex		
Female	9	9
Male	24	24
Primary cancer sites		
Gastric	22	22
Colorectal	3	3
Pancreas	8	8

mal therapeutic strategy in patients with GEP-NEC. Multidetector CT combined with rapid infusion of intravenous contrast medium allows GEP-NEC imaging with high spatial and contrast resolution. Recent studies have demonstrated that dynamic enhanced CT has potential for distinguishing pancreatic NEC from pancreatic ADC, on the basis of duct dilatation [8], and gallbladder NEC from gallbladder ADC, on the basis of tumor morphology and the size of hepatic and lymph node metastases [9]. Studies describing imaging parameters that differentiate between GEP-NEC and GEP-ADC are limited [9, 10]. Therefore, the objective of our study was to assess the capability of contrast-enhanced CT in the differentiation of GEP-NEC and GEP-ADC hepatic metastases.

Materials and methods

Subjects

Our Institutional Review Board approved this retrospective study, and the requirement for informed consent was waived. Consecutive patients attending our institute between January 2009 and February 2016 were eligible for this study. Inclusion criteria were: 1) pathologic diagnosis of NEC, 2) abdominal CT scan within 1 month of pathology, and 3) hepatic metastases identified pathologically or clinically using consecutive imaging or a multi-modality approach (e.g., MRI or positron emission tomography [PET]/CT) by two experienced radiologists (Y-J.S. and Y.C. with 7 and 15 years of experience in abdominal imaging, respectively) in consensus. For comparison, during the same time period and at the same institute, patients with GEP-ADC hepatic metastases were systemically sampled from medical records using random numbers. Inclusion criteria were: (a) pathological diagnosis of GEP-ADC, (b) hepatic metastases identified pathologically or clinically using consecutive imaging or a multi-modality approach (e.g., MRI or positron emission tomography [PET]/CT) by two experienced radiologists (Y-J.S. and Y.C.) in consensus, and (c) unenhanced and contrast-enhanced (hepatic arterial phase and portal venous phase) CT images available. Diagnoses were confirmed by a pathologist (Z-W.L.) with 10 years of experience in gastrointestinal pathology.

CT scan

CT scans were performed using multidetector CT scanners (LightSpeed VCT or Discovery 750HD, GE Healthcare, Milwaukee, WI, or iCT, Philips Healthcare). The scanning parameters were: tube voltage 120-kV; automatic tube current modulation, detector collimations of 0.625 mm, and a pitch of 0.98-1.2. Images with 5-mm-thick sections were acquired. The size of the scan field of view was adapted to each individual's physique. A pre-contrast scan was obtained prior to the intravenous administration of 2.0 mL/kg of nonionic contrast material (iopromide, Ultravist 300, Bayer Schering Palmar Berlin, Germany, or Omnipaque 300; Nycomed, Princeton, NJ, USA) followed by a 20 mL saline chaser bolus injected at a rate of 3 mL/sec. Using fixed scan delay, the hepatic arterial phase scan was started 25-30 seconds after the initiation of the contrast material injection. The portal venous phase scan was obtained 50-55 seconds after the end of the hepatic arterial phase scan.

Image analysis

The following parameters were qualitatively evaluated: 1) tumor distribution, defined as focal (confined to one liver lobe or two adjacent segments) or diffuse (multifocal hepatic metastases); 2) the presence or absence of tumor-feeding arteries and intratumoral neovascularity; and 3) dynamic enhancement patterns, based on visual estimation of changes between the hepatic arterial phase and portal venous phase. Enhancement patterns were defined as plateaued if tumors were homogeneous on hepatic arterial phase and portal venous phase images; progressive if enhancement of tumors on portal venous phase images was greater than on hepatic arterial phase images; or wash-

Table 2. Qualitative parameters characterizing GEP-NEC and GEP-ADC hepatic metastases on CT

Parameter	NEC hepatic metastases	ADC hepatic metastases	χ^2	*p*
Distribution			0.407	0.523
Focal	5 (15.2%)	7 (21.2%)		
Diffuse	28 (84.8%)	26 (78.8%)		
Feeding artery			8.800	0.003
Presence	24 (72.7%)	12 (36.4%)		
Absence	9 (27.3%)	21 (63.6%)		
Intra-tumoral Neovascularity			15.015	<0.001
Presence	19 (57.6%)	4 (12.1%)		
Absence	14 (42.4%)	29 (87.9%)		
Dynamic enhancement pattern			12.835	0.002
Plateau	14 (42.4%)	28 (84.8%)		
Progressive	15 (45.5%)	4 (12.1%)		
Washout	4 (12.1%)	1 (3.0%)		

out if enhancement of tumors on portal venous phase images was less than on hepatic arterial phase images. Patients with multiple tumors were defined according to the features that characterized the majority of the lesions.

The following parameters were quantitatively evaluated: 1) tumor size, determined by measuring the largest diameter on axial images; 2) number of tumors, recorded as <20 or defined as uncountable if >20; 3) CT attenuation of the largest lesion in each patient and the surrounding liver parenchyma, measured by drawing regions of interest (ROIs) on pre- and post-contrast hepatic arterial phase and portal venous phase images. The ROI for each lesion was placed on the section with the largest lesion diameter and a maximum oval or round area devoid of necrosis. CT attenuation of the adjacent liver parenchyma was measured with an ROI ≤10 mm in diameter that was devoid of vascular structures. The enhancement ratio of the lesion versus the surrounding liver parenchyma in the hepatic arterial phase (T-L/A) and portal venous phase (T-L/P) were calculated as: Enhancement ratio = CT value of lesion/CT value of liver.

Qualitative analysis was performed by two body CT radiologists (Y-J.S. and Y.C.) who had 7 years and 15 years of experience in abdominal imaging, respectively. The reviewers were blinded to the clinical and pathological data. Discrepancies between the radiologists' findings were resolved by discussion until consensus was reached. The size, number, and CT attenuation measurements were conducted by one radiologist (Y.C.).

Data analyses

All statistical analyses were performed using the SPSS software package (version 16.0, SPSS Inc., Chicago, IL, USA). Fisher's exact test for categorical variables and the independent t-test for continuous variables were used to compare the features of GEP-NEC hepatic metastases and GEP-ADC hepatic metastases on CT images. Thereafter, binary logistic regression analyses were performed to determine the most predictable findings. Receiver operating characteristic (ROC) curve analysis was conducted to ascertain optimal cut-off values for differentiating GEP-NEC hepatic metastases from GEP-ADC hepatic metastases. The Kappa statistic was used to evaluate inter-observer agreement. A *p* value <0.05 was considered statistically significant.

Results

Eighty-nine consecutive patients were eligible for inclusion in this study. Among these, 12 patients were excluded as the primary cancer was of unknown origin or was not GEP, 20 patients were treated before the CT scan, 20 patients had composite tumors (e.g., mixed adenoneuroendocrine carcinoma), and 4 patients had poor image quality. Finally, 33 patients with GEP-NEC hepatic metastases were matched to 33 patients with GEP-NEC hepatic metastases for age, sex, and primary cancer site. Patients' demographic and clinical characteristics are shown in **Table 1**.

Qualitative CT findings are summarized in **Table 2**. Inter-observer agreement among the CT radiologists was good for tumor distribution (kappa, 0.796), presence of a feeding artery (kappa, 0.789), presence of intratumoral neovascularity (kappa, 0.710), and assessment of the dynamic enhancement pattern (kappa, 0.660). Univariate analyses revealed that both GEP-NEC and GEP-ADC hepatic metastases

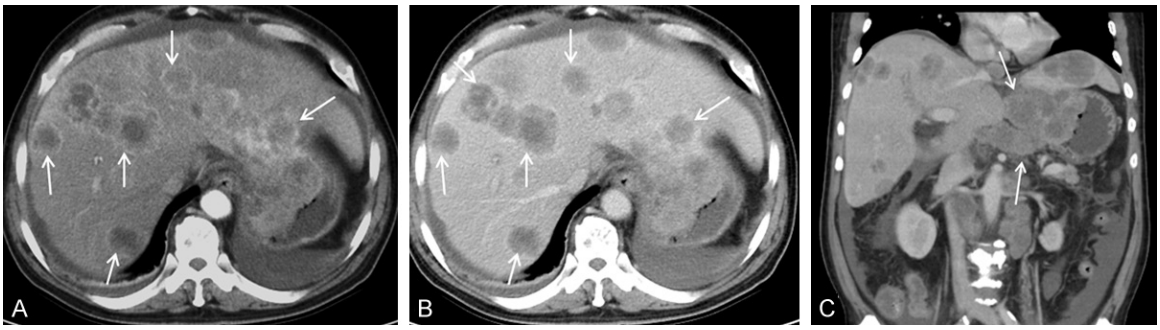

Figure 1. A 63-year-old man with gastric NEC: (A) Hepatic arterial phase CT image showing multiple peripheral hyper-enhanced hepatic metastases (arrows); (B) Portal venous phase CT image showing decreased enhancement and areas of washout (arrows); (C) Portal venous phase coronal CT image showing lymphadenopathy (arrows).

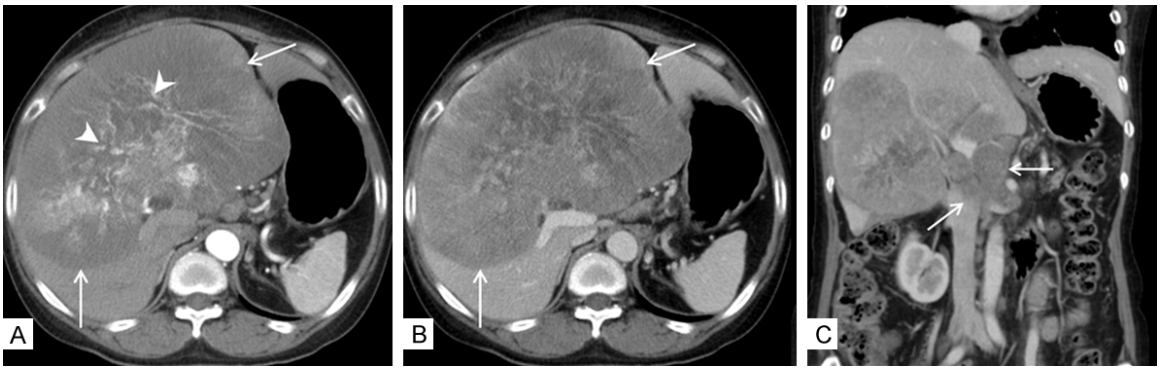

Figure 2. A 53-year-old woman with pancreatic NEC: (A) Hepatic arterial phase axial CT image showing a hepatic metastasis (arrows) with heterogeneous hyper-enhancement and intra-tumoral neovascularity (arrowheads); (B) Portal venous phase CT image showing iso-to hypo enhancement and areas of washout (arrows). (C) Portal venous phase CT image showing lymphadenopathy (arrows).

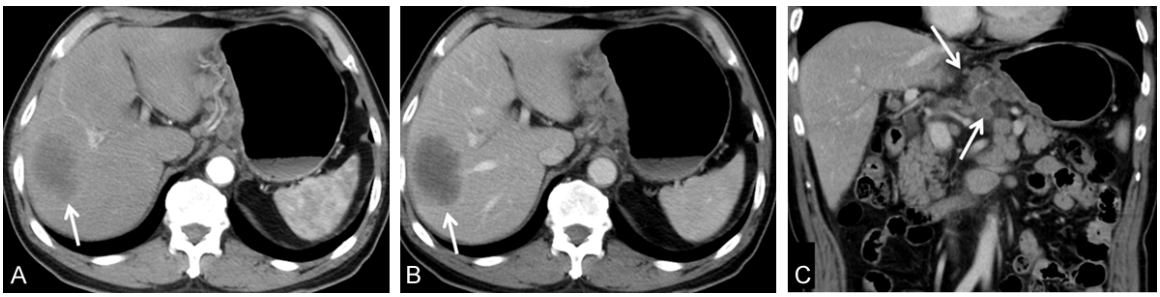

Figure 3. A 66-year-old man with gastric adenocarcinoma: (A) Hepatic arterial phase axial CT image showing a hypo-enhanced hepatic metastasis in the right lobe of the liver (arrow) and regional lymphadenopathy (arrowhead) next to the lesser gastric curvature. (B) Portal venous phase CT image showing hypo-enhancement and plateau enhancement (arrow). (C) Portal venous phase coronal CT image showing regional lymphadenopathy (arrows) next to the lesser gastric curvature.

tended to show diffuse distribution (84.8% vs. 78.8%, p=0.532). However, there was a significantly higher prevalence of tumor feeding arteries (72.7% vs. 36.4%, p=0.003) and intratumoral neovascularity (57.6% vs. 12.1%, p<0.001) in GEP-NEC hepatic metastases than GEP-ADC hepatic metastases, and there was a significant difference in the dynamic enhancement pattern (p=0.002) (**Figures 1**-**4**).

Quantitative CT findings are shown in **Table 3**. The mean T-L/A in GEP-NEC hepatic metasta-

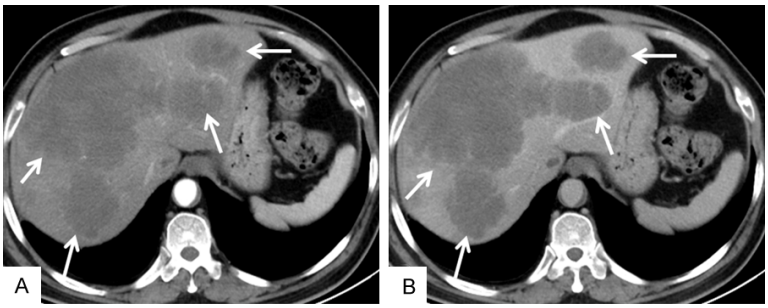

Figure 4. A 68-year-old man with rectal adenocarcinoma: (A) Hepatic arterial phase CT image showing multiple hypo-enhanced hepatic metastases; (B) Portal venous phase CT image showing hypo-enhancement and plateau enhancement (arrows).

Table 3. Quantitative parameters characterizing GEP-NEC and GEP-ADC hepatic metastases on CT

Parameter	NEC hepatic metastases	ADC hepatic metastases	t	*p*
Number	14.30±10.00	12.91±10.44	0.582	0.554
Size (mm)	55.03±39.22	41.30±25.87	1.679	0.098
T-L/A	0.90±0.24	0.72±0.19	3.362	0.001
T-L/P	0.68±0.15	0.60±0.17	1.934	0.058

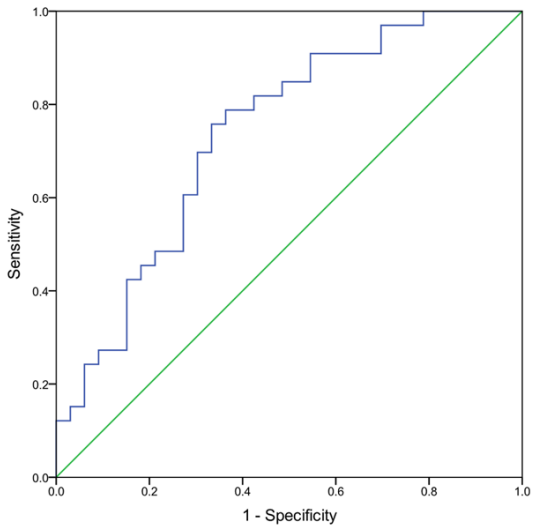

Figure 5. Receiver operating characteristic curves of T-L/A for predicting GEP-NEC hepatic metastases.

ses was significantly higher than GEP-ADC hepatic metastases (0.90±0.24 vs. 0.72±0.19, p=0.001); there were no significant differences in tumor size (p=0.098), tumor number (p= 0.554), or T-L/P (p=0.058).

Binary regression analysis identified the presence of intratumoral neovascularity as the only independent predictor of GEP-NEC hepatic metastases on CT (odds ratio=7.097; 95% CI=1.852-27.196; p=0.004). ROC analysis demonstrated that the optimal T-L/A cutoff value for predicting GEP-NEC hepatic metastasis was 0.75 with an area under the curve of 0.737, sensitivity of 75.8%, and specificity of 66.7% (**Figure 5**).

Discussion

This retrospective study compared qualitative and quantitative imaging parameters to differentiate between GEP-NEC and GEP-ADC hepatic metastases on contrast-enhanced CT. A univariate analysis revealed a significant difference in three qualitative parameters, the presence of tumor-feeding arteries (intratumoral neovascularity, and degree of hepatic arterial enhancement) and one quantitative parameter (T-L/A) between GEP-NEC and GEP-ADC hepatic metastases. Binary regression analysis identified the presence of intratumoral neovascularity as the only independent predictor of GEP-NEC hepatic metastases on CT. Taken together, these findings suggest that GEP-NEC hepatic metastases may be differentiated from GEP-ADC hepatic metastases on CT based on the presence of intratumoral neovascularity and greater enhancement on hepatic arterial phase images. To the author's knowledge, this is the first article to identify the CT features that enable differentiation between GEP-NEC and GEP-ADC hepatic metastases.

The current study demonstrated that the presence of intratumoral vessels is the best discriminator between GEP-NEC and GEP-ADC hepatic metastases on CT; 57.6% of patients with GEP-NEC hepatic metastases showed intratumoral vessels compared to 12.1% of GEP-ADC hepatic metastases. The presence of large intratumoral vessels may reflect the high vascularity of GEP-NEC hepatic metastases. Generally, NEC hepatic metastases are characterized by a high vascular density, resulting in a hyper-vascular appearance on imaging, while

GEP-ADC hepatic metastases are hypo-vascular [11]. In our study, the higher vascularity of GEP-NEC hepatic metastases was confirmed by the high degree of hepatic arterial enhancement. Furthermore, the mean T-L/A was significantly higher in the GEP-NEC hepatic metastases compared to the GEP-ADC hepatic metastases (0.90 vs. 0.72). Evidence suggests that large NEC hepatic metastases are associated with well-developed peri-tumoral vessels and contain large irregular vascular channels [12]. The high prevalence of feeding arteries in GEP-NEC hepatic metastases may be related to their high vascularity. Accordingly, a previous study reported that the presence of large intratumoral vessels was correlated with a higher degree of angiogenesis in gastrointestinal stromal tumors [13].

GEP-NEC and GEP-ADC hepatic metastases showed different contrast enhancement patterns on CT. In the current study, 45.5% and 42.4% of GEP-NEC hepatic metastases showed progressive and plateau enhancement, respectively, whereas 84.8% of GEP-ADC showed plateau enhancement. We speculate that these different enhancement patterns may be explained by the difference in vascularity between GEP-NEC and GEP-ADC hepatic metastases. Our findings are in agreement with previous reports showing that GEP-ADC hepatic metastases are hypo-vascular [11, 14], with faint or negligible enhancement in hepatic arterial phase images and isointense, negligible, or incomplete central progression on portal venous and delay phase images [15]. Kim et al. reported that both primary gallbladder NEC and hepatic metastases showed significantly stronger enhancement in the late arterial phase than gallbladder ADCs [9], and gastric NEC hepatic metastases had a higher metastasis-to-liver ratio than gastric ADC hepatic metastases [10].

The current study has several limitations. First, because of its retrospective nature, there was potential selection bias in the patient sample. Second, a fixed delay time was used to trigger the start of the scans instead of bolus tracking. However, our findings represent robust evidence as we used a delay time recommended by consensus guidelines [16], cases with inadequate image quality were excluded, and enhancement ratios were used for quantitative comparison.

In conclusion, this study compared qualitative and quantitative imaging parameters to differentiate between GEP-NEC and GEP-ADC hepatic metastases on contrast-enhanced CT. Intratumoral neovascularity was identified as the most useful parameter for differentiating between GEP-NEC and GEP-ADC hepatic metastases on CT. Contrast-enhanced CT may have clinical application in the differential diagnosis of GEP-NEC and GEP-ADC hepatic metastases.

Acknowledgements

This study was supported by National Natural Science Foundation of China (No. 6152010-6004, and No. 81641170).

Disclosure of conflict of interest

None.

Address correspondence to: Dr. Ying-Shi Sun, Department of Radiology, Key Laboratory of Carcinogenesis and Translational Research (Ministry of Education), Peking University Cancer Hospital & Institute, 52 Fucheng Road, Haidian District, Beijing 100142, China. Tel: 86-10-88196822; Fax: 86-10-88196031; E-mail: sys27@163.com

References

[1] Hallet J, Law CH, Cukier M, Saskin R, Liu N and Singh S. Exploring the rising incidence of neuroendocrine tumors: a population-based analysis of epidemiology, metastatic presentation, and outcomes. Cancer 2015; 121: 589-597.

[2] Hassan MM, Phan A, Li D, Dagohoy CG, Leary C and Yao JC. Risk factors associated with neuroendocrine tumors: A U.S.-based case-control study. Int J Cancer 2008; 123: 867-873.

[3] Yao JC, Hassan M, Phan A, Dagohoy C, Leary C, Mares JE, Abdalla EK, Fleming JB, Vauthey JN, Rashid A and Evans DB. One hundred years after "carcinoid": epidemiology of and prognostic factors for neuroendocrine tumors in 35,825 cases in the United States. J Clin Oncol 2008; 26: 3063-3072.

[4] Pavel M, Baudin E, Couvelard A, Krenning E, Öberg K, Steinmüller T, Anlauf M, Wiedenmann B, Salazar R; Barcelona Consensus Conference participants. ENETS consensus guidelines for the management of patients with liver and other distant metastases from neuroendocrine neoplasms of foregut, midgut, hindgut, and unknown primary. Neuroendocrinology 2012; 95: 157-176.

[5] Pape UF, Berndt U, Muller-Nordhorn J, Bohmig M, Roll S, Koch M, Willich SN and Wiedenmann

B. Prognostic factors of long-term outcome in gastroenteropancreatic neuroendocrine tumours. Endocr Relat Cancer 2008; 15: 1083-1097.

[6] Ahmed A, Turner G, King B, Jones L, Culliford D, McCance D, Ardill J, Johnston BT, Poston G, Rees M, Buxton-Thomas M, Caplin M and Ramage JK. Midgut neuroendocrine tumours with liver metastases: results of the UKINETS study. Endocr Relat Cancer 2009; 16: 885-894.

[7] Strosberg JR, Coppola D, Klimstra DS, Phan AT, Kulke MH, Wiseman GA, Kvols LK; North American Neuroendocrine Tumor Society (NANETS). The NANETS consensus guidelines for the diagnosis and management of poorly differentiated (high-grade) extrapulmonary neuroendocrine carcinomas. Pancreas 2010; 39: 799-800.

[8] Kim JH, Eun HW, Kim YJ, Lee JM, Han JK and Choi BI. Pancreatic neuroendocrine tumour (PNET): staging accuracy of MDCT and its diagnostic performance for the differentiation of PNET with uncommon CT findings from pancreatic adenocarcinoma. Eur Radiol 2016; 26: 1338-1347.

[9] Kim TH, Kim SH, Lee KB and Han JK. Outcome and CT differentiation of gallbladder neuroendocrine tumours from adenocarcinomas. Eur Radiol 2017; 27: 507-517.

[10] Kim SH, Kim SH, Kim MA, Shin CI, Han JK and Choi BI. CT differentiation of poorly-differentiated gastric neuroendocrine tumours from well-differentiated neuroendocrine tumours and gastric adenocarcinomas. Eur Radiol 2015; 25: 1946-1957.

[11] Nino-Murcia M, Olcott EW, R. Brooke Jeffrey J, Lamm RL, Beaulieu CF and Jain KA. Focal liver lesions: pattern-based classification scheme for enhancement at arterial phase CT. Radiology 2000; 215: 746-751.

[12] Pourreyron C, Poncet G, Roche C, Gouysse G, Nejjari M, Walter T, Villaume K, Jacquier MF, Bernard C, Dumortier J, Chayvialle JA, Bachelot T and Scoazec JY. The role of angiogenesis in endocrine liver metastases: an experimental study. J Surg Res 2008; 144: 64-73.

[13] Yamashita Y, Kato J, Ueda K, Nakamura Y, Abe H, Tamura T, Itonaga M, Yoshida T, Maeda H, Moribata K, Niwa T, Maekita T, Iguchi M, Tamai H and Ichinose M. Contrast-enhanced endoscopic ultrasonography can predict a higher malignant potential of gastrointestinal stromal tumors by visualizing large newly formed vessels. J Clin Ultrasound 2015; 43: 89-97.

[14] Danet IM, Semelka RC, Nagase LL, Woosely JT, Leonardou P and Armao D. Liver metastases from pancreatic adenocarcinoma: MR imaging characteristics. J Magn Reson Imaging 2003; 18: 181-188.

[15] Danet IM, Semelka RC, Leonardou P, Braga L, Vaidean G, Woosley JT and Kanematsu M. Spectrum of MRI appearances of untreated metastases of the liver. AJR Am J Roentgenol 2003; 181: 809-817.

[16] Sundin A, Vullierme MP, Kaltsas G and Plockinger U. ENETS consensus guidelines for the standards of care in neuroendocrine tumors: radiological examinations. Neuroendocrinology 2009; 90: 167-183.